

Stereochemical and Skeletal Diversity
Arising from Amino Propargylic AlcoholsDaniela Pizzirani,[‡] Taner Kaya,[†] Paul A. Clemons,[†] and Stuart L. Schreiber^{*,†}

Howard Hughes Medical Institute, Broad Institute of Harvard and MIT, 7 Cambridge Center, Cambridge, Massachusetts 02142, and Department of Chemistry and Chemical Biology, Harvard University, Cambridge, Massachusetts 02138

stuart_schreiber@harvard.edu

Received April 21, 2010

ABSTRACT



An efficient synthetic pathway to the possible stereoisomers of skeletally diverse heterocyclic small molecules is presented. The change in shape brought about by different intramolecular cyclizations of diastereoisomeric amino propargylic alcohols is quantified using principal moment-of-inertia (PMI) shape analysis.

Human genetics and physiology are increasingly revealing the root causes of human disorders, yet many of the relevant targets and processes are considered difficult to modulate with small molecules.^{1,2} At least part of the difficulty is associated with the candidate small molecules that populate screening collections.³ We describe an effort to address this shortcoming by applying a build/couple/pair strategy in organic synthesis.^{4,5} The synthetic pathway we describe focused on the goal of synthesizing stereoisomers of skeletally diverse compounds so that stereochemistry-based structure–activity relationships (SARs) can be derived directly from small-molecule screening. Small-molecule probe-development efforts are significantly enhanced when “hits” from screens can be prioritized and optimized using stereochemistry-based SARs, and we imagine that drug discovery efforts might similarly be facilitated in the future.

We envisioned that densely functionalized chiral amino propargylic alcohols **1a–d** could be synthesized as a complete

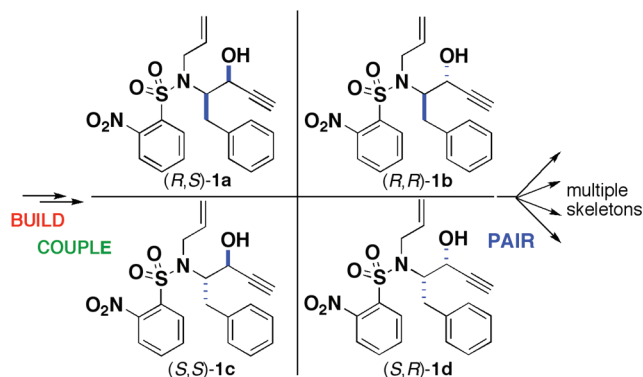


Figure 1. Stereochemical and skeletal diversity.

matrix of stereoisomers using simple coupling reactions and readily available building blocks. These coupling products undergo intramolecular cyclization reactions to generate diverse heterocyclic skeletons in 1–2 steps (Figure 1).

[†] Broad Institute of Harvard and MIT.

[‡] Harvard University. Current address: Department of Drug Discovery and Development, Italian Institute of Technology (IIT), Via Morego 30, 16163 Genova, Italy.

(1) Schreiber, S. L. *ChemBioChem* **2009**, *10*, 26–29.

(2) Schreiber, S. L. *Nature* **2009**, 153–154.

(3) Payne, D. J.; Gwynn, M. N.; Holmes, D. L.; Pompliano, D. L. *Nat. Rev. Drug Discovery* **2007**, *6*, 29–40.

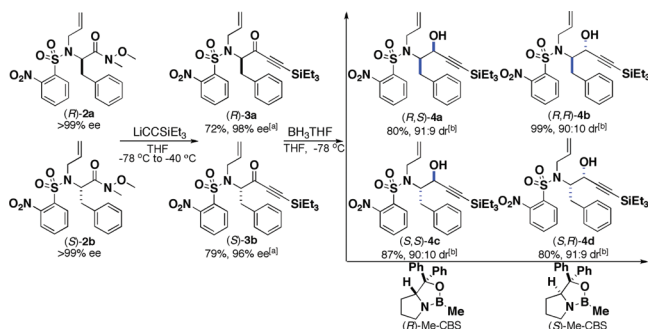
(4) Nielsen, T. E.; Schreiber, S. L. *Angew. Chem., Int. Ed.* **2008**, *47*, 48–56.

(5) For recent examples, see: (a) Kumagai, N.; Muncipinto, G.; Schreiber, S. L. *Angew. Chem. Int. Ed.* **2006**, *45*, 3635–3638. (b) Spiegel, D. A.; Schroeder, F. C.; Duvall, J. R.; Schreiber, S. L. *J. Am. Chem. Soc.* **2006**, *128*, 14766–14767. (c) Uchida, T.; Rodriguez, M.; Schreiber, S. L. *Org. Lett.* **2009**, *11*, 1559–1562.

We initiated our study with the preparation of densely functionalized amides **2a,b**⁶ starting from commercial (*R*)- and (*S*)-phenylalanine.⁷ The 2-nitrobenzylsulfonyl (Ns) group was chosen both to modulate the pK_a of the attached nitrogen to facilitate subsequent allylation⁸ and to introduce an additional chemical handle for the “pair phase” of the pathway.

In the couple phase, an alkynyl moiety was incorporated by triethylsilylacetylide addition to amides **2a,b**, generating the corresponding α,β -acetylenic ketones **3a,b** in good yield and without racemization, when temperature and reaction time were optimized (Scheme 1). Reactions that enable

Scheme 1. Synthesis of Diastereoisomeric Amino Propargylic Alcohols



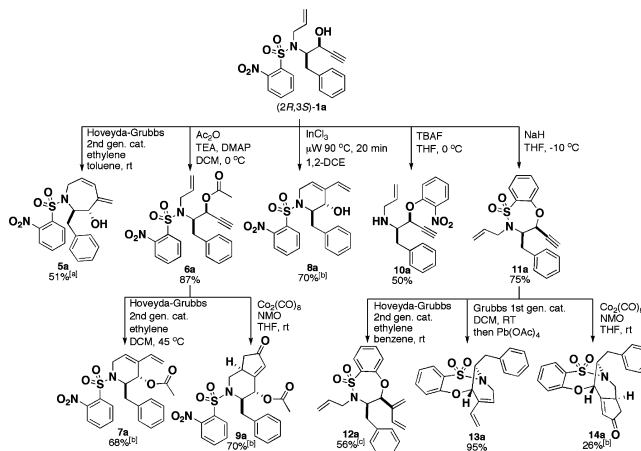
^a ee was determined by SFC analysis. ^b dr was determined by ¹H NMR analysis of the inseparable mixture of the two diastereomers.

controlled access to all possible diastereomers are especially valuable in diversity-oriented synthesis.⁹ After extensive experimentation, we determined that the carbonyl diastereotopic faces in (*R*)-**3a** and (*S*)-**3b** can be differentiated efficiently by the chirality of CBS-Me-oxazaborolidine,¹⁰ overriding the influence of the adjacent nitrogen-substituted stereogenic center. The reduction of chiral ynone (*R*)-**3a** (98% ee) using the stoichiometric complex (*R*)-Me-CBS-oxazaborolidine/BH₃·THF in dry THF at -78 °C delivered the *syn*-amino propargylic alcohol (*2R,3S*)-**4a** in excellent yield and good diastereoselectivity (diastereoisomeric ratio dr = 91:9). When (*R*)-**3a** was instead reduced with (*S*)-Me-CBS-oxazaborolidine/BH₃·THF, the corresponding *anti*-amino propargylic alcohol (*2R,3R*)-**4b** was obtained in comparable yield and diastereoselectivity. Reduction of (*S*)-**3b** (96% ee) under the same reaction conditions provided (*2S,3S*)-**4c** and (*2S,3R*)-**4d**, respectively (Scheme 1). In contrast, reduction of (*R*)-**3a** with NaBH₄ in MeOH afforded a 5:1 mixture of *anti/syn* diastereoisomeric alcohols. Desilylation with a 1:1 molar ratio of TBAF/AcOH efficiently delivered the key intermediates of the pathway **1a–d**.¹¹ The diastereoisomeric ratio for the *anti*-products (*2R,3R*)-**1b** and (*2S,3S*)-**1c** was increased to 97:3 after a single crystallization.

We next explored a series of intramolecular cyclization reactions using the *syn*- and *anti*-diastereomers **1a,b**¹² (based on symmetry, we expect that the same reactions would work analogously on enantiomers **1c,d**, providing products in all stereochemical combinations). Skeletal diversification was

achieved by reagent- and substrate-controlled site-selective activation of different pairs of functional groups, strategically placed on the linear template **1a** (Scheme 2). We first

Scheme 2. Skeletal Diversity through Functional Group Pairing Reactions



^a Ratio *endo/exo* = 10:1.5 was determined by ¹H NMR. ^b Single stereoisomer. ^c Intramolecular enyne metathesis product **13a** was also obtained as minor product in 38% yield.

investigated enyne metathesis to access a substituted vinyl tetrahydropyridine-type skeleton, which is poised for further diversification. We determined that *syn*-amino propargylic alcohol (*2R,3S*)-**1a** in the presence of second generation Hoveyda–Grubbs catalyst (5 mol %) under ethylene atmosphere undergoes *endo*-mode selective cyclization forming the corresponding cycloheptadiene **5a** as the major regioisomer (*endo/exo* selectivity = 10:1.5).¹³ Noting the size of the newly formed ring and the presence of nonsubstituted alkenyl and alkynyl groups in the substrate,¹⁴ we determined that this unusual result was influenced by the free hydroxyl group at the propargylic position. Protection of the alcohol as acetate **6a** resulted in *exo*-mode ring closure to form six-membered ring diene **7a** as the only product. We speculate that in the latter case the *endo*-mode RCM is disfavored as a result of the formation of a sterically hindered alkylidene, compared to the *exo*-mode RCM intermediate. Under the same reaction conditions, the *anti*-diastereomer (*2R,3R*)-**1b**

(6) Experimental procedures to amide derivatives **2a,b** are reported in Supporting Information.

(7) D'Aniello, F.; Mann, A. *J. Org. Chem.* **1996**, *61*, 4870–4871.

(8) Fukuyama, T.; Jow, C.-K.; Cheung, M. *Tetrahedron Lett.* **1995**, *36*, 6373–6374.

(9) For examples, see: (a) Taylor, M. S.; Jacobsen, E. N. *Proc. Natl. Acad. Sci. U.S.A.* **2004**, *101*, 5368–5373. (b) Balskus, E. P.; Jacobsen, E. N. *Science* **2007**, *317*, 1736–1740. (c) Liu, X.; Henderson, J. A.; Sasaki, T.; Kishi, Y. *J. Am. Chem. Soc.* **2009**, *131* (46), 16678–16680.

(10) Corey, E. J.; Helal, C. J. *Angew. Chem., Int. Ed.* **1998**, *37*, 1986–2012.

(11) Yohannes, D.; Danishefsky, S. *J. Tetrahedron Lett.* **1992**, *33*, 7469–7462.

(12) Structures and stereochemistry of all the reported compounds were determined by detailed spectroscopic analysis, including X-ray structures of compounds **11a**, **13a**, and **14a** (see Supporting Information).

(13) *Endo/exo* products ratio was determined by ¹H NMR analysis of the inseparable mixture of the two regioisomers.

yielded a mixture of decomposition products, whereas the corresponding propargylic acetate **6b** delivered **7b** in moderate yield as a single stereoisomer (Figure 2).¹⁵ Gratifyingly,

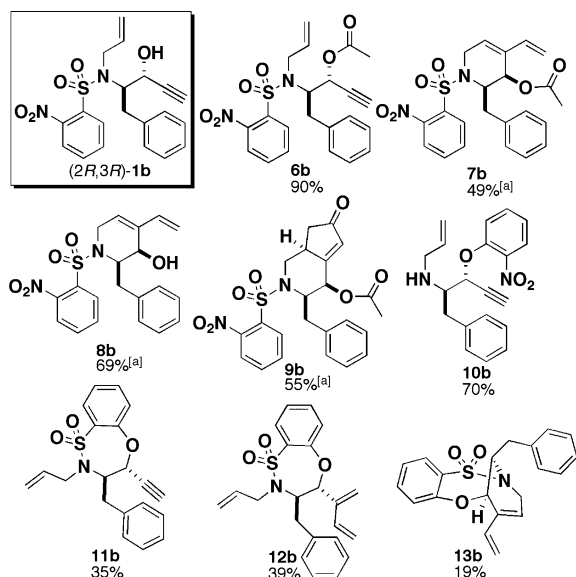


Figure 2. Skeletal diversity from *anti*-amino propargylic alcohol **1b**. Note: ^asingle stereoisomer.

we found that catalytic InCl_3 (15 mol %) promoted skeletal reorganization¹⁶ of both *syn*- and *anti*-diastereomers **1a,b** under microwave conditions, providing the corresponding dienes **8a,b** as single products in good yield. We investigated the Pauson–Khand reaction (PKR) as an additional alkyne–alkene functional group-pairing reaction. After conversion of amino propargylic alcohol **1a** to acetate **6a**, the $\text{Co}_2(\text{CO})_8$ complex derived from **6a** was treated with *N*-methylmorpholine *N*-oxide¹⁷ at room temperature to provide cyclopenten-2-enone derivative **9a** with excellent stereoselectivity. Similarly, diastereomer **6b** formed PKR product **9b** stereoselectively. The stereochemistry of **9a** and **9b** was determined by NOE analyses.¹² The benzyl substituent influenced the diastereofacial control of cyclization, whereas the acetoxy-substituted stereogenic center provided virtually no directing effect.

We next examined polar/polar functional group-pairing reactions for further skeletal diversification (Scheme 2). Treatment of **1a** with tetrabutylammonium fluoride (TBAF) in THF at 0 °C provided the Smiles rearrangement¹⁸ product **10a** in

50% yield. In contrast, *anti*-diastereomer **1b** rearranged to **10b** with high site-selectivity in presence of diaza-(1,3)-bicyclo[5.4.0]undecane (DBU) in refluxing THF. When **1a** was treated with NaH in THF, the resultant alkoxide participated in endocyclic nucleophilic aromatic substitution¹⁹ to yield the seven-membered benzothiazepine derivative **11a**. Control of the temperature between –10 and 0 °C was needed to obtain **11a** selectively in 75% yield. In contrast, *anti*-diastereomer (*2R,3R*)-**1b** only reacted at room temperature under these conditions, generating (*3R,4R*)-**11b** in moderate yield due to lower selectivity of the *ipso*-substitution relative to the Smiles rearrangement.²⁰

To access wider skeletal diversity, we sought to take advantage of the nonpolar chemical handles still available on the benzothiazepine core **11a**. An enyne metathesis reaction yielded cross-metathesis product **12a** in the presence of ethylene gas. Intramolecular enyne metathesis product **13a** was obtained selectively in excellent yield by simply treating the substrate with first-generation Grubbs catalyst (3 mol %) in dichloromethane at room temperature followed by addition of lead tetraacetate (15 mol %). The latter was added to scavenge ruthenium and phosphine impurities.²¹ The structure of the bridged ten-membered ring diene was confirmed by X-ray analysis.¹² Diastereomer **11b** only reacted in the presence of ethylene gas providing the cross-metathesis product **12b** as the major adduct and cyclic diene **13b** in combined 58% yield. Skeletal diversification via PKR on **11a** afforded bridged ten-membered ring cyclopenten-2-enone derivative **14a** in moderate yield as a single stereoisomer. X-ray structure analysis confirmed the stereochemistry of this product.¹² Diastereomer **11b** did not undergo the PKR.

We sought to quantify the extent to which the aforementioned intramolecular cyclizations access different overall molecular shapes. To obtain a simple assessment of diversity in molecular shape among the compounds studied, we calculated normalized principal moment-of-inertia (PMI) ratios,²² plotted as two-dimensional characteristic coordinates ($I_{\text{small}}/I_{\text{large}}$, $I_{\text{medium}}/I_{\text{large}}$) for compounds **1a** and **5a–14a** (Figure 3A). Points in the resulting graph occupy an isosceles triangle defined by the vertices (0,1), (0.5,0.5), and (1,1), corresponding to the shapes of rod, disk, and sphere, respectively.

For **1a** and **5a–14a**, we observe a band covering the space between the rod- and disk-like regions of the PMI space; **1a** is centrally located in this band, and its direct reaction products, **5–6a**, **8a**, and **10–11a**, span nearly the range of rod- and disk-like shapes among all 11 compounds. However, further cyclization of **6a** to produce **7a** and **9a** results in the two most disk-like of all 11 compounds, though each is similar in shape to its precursor **6a**. Further reaction of **11a** to produce **12–14a** similarly results in the three most sphere-like among the 11 compounds. In contrast to cyclization of **6a**, these modifications of **11a** result in relatively large overall changes in shape.

(14) For the definition of *endo/exo*-mode selectivity in enyne RCM and recent examples, see: (a) Hansen, E. C.; Lee, D. *Acc. Chem. Res.* **2006**, *39*, 509–519. (b) Lee, Y.-J.; Schrock, R. R.; Hoveyda, A. H. *J. Am. Chem. Soc.* **2009**, *131*, 10652–10661. (c) Hansen, E. C.; Lee, D. *J. Am. Chem. Soc.* **2003**, *125*, 9582–9583.

(15) Experimental reaction conditions to obtain skeletons **6–13b** are reported in Supporting Information.

(16) (a) Lee, S. I.; Chatani, N. *Chem. Commun.* **2009**, 371–384. (b) Miyahana, Y.; Chatani, N. *Org. Lett.* **2006**, *8*, 2155–2158.

(17) Shambayati, S.; Crowe, W. E.; Schreiber, S. L. *Tetrahedron Lett.* **1990**, *31*, 5289–5292.

(18) Yeom, C.-E.; Kim, H. W.; Lee, S. Y.; Kim, B. M. *Synlett* **2007**, *1*, 146–150.

(19) Kleb, K. G. *Angew. Chem., Int. Ed.* **1968**, *7*, 291.

(20) Zhou, A.; Rayabarapu, D.; Hanson, P. R. *Org. Lett.* **2009**, *11*, 531–534.

(21) Paquette, L. A.; Schloss, J. D.; Efremov, I.; Fabris, F.; Gallou, F.; Mendez-Andino, J.; Yang, J. *Org. Lett.* **2000**, *2*, 1259–1261.

(22) Sauer, W. H.; Schwarz, M. K. *J. Chem. Inf. Comput. Sci.* **2003**, *43*, 987–1003.

We also used PMI ratio analysis to quantify the extent to which diastereomeric products **1b** and **6b–13b** differ from their counterparts **1a** and **6a–13a** (Figure 3B). We quantified the PMI distance between matched pairs and observed the largest such differences for compounds **12a,b** ($d_{a-b} = 0.364$), **11a,b** ($d_{a-b} = 0.211$), and **10a,b** ($d_{a-b} = 0.116$). Interestingly, for **11** and **12**, the **a** diastereomer is more disk-like, which may be due to extended conformations of acyl and allyl groups perpendicular to the rod-like structure of the molecule, whereas **b** is more rod-like; the converse is true for **10**, where an opposite relationship is observed. The minimum difference we observed was for the pair of amino propargylic alcohols **1a,b** ($d_{a-b} = 0.008$), which makes sense due to the short, linear hydroxyl substituent at one of the stereocenters. A

similar trend was observed for other compounds with small substituents, e.g., in the case of **13a,b**, where only the hydrogen atom at the bridge position is inverted.

To compare additional compounds prospectively available from this chemistry to compounds from other sources (Figure 3C), we enumerated a virtual library of compounds that would be obtained by substituting starting phenylalanines with alternative amino acids to give 6 additional R-groups (bromobenzyl, hydroxymethyl, *o*-TBS-ethyl, *p*-hydroxybenzyl, *p*-azidobenzyl, hydroxyethyl) at carbon 2. We compared the resulting 140-compound library to 140 diverse compounds selected²³ from each of two sources: commercial compounds (CC) typical of those found in many screening collections and natural products (NP).²⁴ We note that CC compounds cover the left edge of the PMI space, taking shapes intermediate between rods and discs, whereas NP compounds distribute more evenly over the space and populate the intermediate region between disk- and sphere-like shapes. By comparison, the virtual products from this chemistry also provide more broad coverage of the space and include several products among the most sphere-like of all compounds compared.

We initiated this research with the hypothesis that accessing stereoisomers of skeletally diverse compounds will facilitate small-molecule probe and drug discovery efforts. This new DOS pathway will enable further testing of this hypothesis. This work also provides a framework for understanding the consequences of different synthetic decisions in the “pair phase” of build/couple/pair synthesis strategies using PMI shape analysis to understand changes in shape brought about by different intramolecular cyclizations. The analysis of small-molecule screening results using these compounds should enable us to link shape analyses and synthetic decisions to biological assay outcomes in the future.

Acknowledgment. The NIGMS-sponsored Center of Excellence in Chemical Methodology and Library Development (P50-GM069721) enabled this research. We are grateful to Dr. Peter Muller at MIT for X-ray crystallographic analysis, and Emeline Tissot and Christopher Johnson at the Broad Institute for help with SFC/MS. D.P. thanks Yikai Wang and Dr. Giovanni Muncipinto at the Department of Chemistry and Chemical Biology (Harvard University), Dr. Manuela Rodriguez currently at the Department of Pharmacological Sciences (University of Salerno), and Dr. Masaaki Hirano currently at Astellas Pharma Inc. for helpful discussions. S.L.S. is an investigator with the Howard Hughes Medical Institute.

Supporting Information Available: Experimental procedures and full spectroscopic data for all new compounds. This material is available free of charge via the Internet at <http://pubs.acs.org>.

OL100914B

(23) Diverse selections were made from a larger collection using the “Diverse Molecules” component of Pipeline Pilot (SciTegeic, Inc.) and the ECFP4 molecular fingerprints.

(24) Clemons, P. A.; Bodycombe, N. E.; Carrinski, H. A.; Wilson, J. A.; Wagner, B. K.; Koehler, A. N.; Schreiber, S. L. Manuscript submitted.

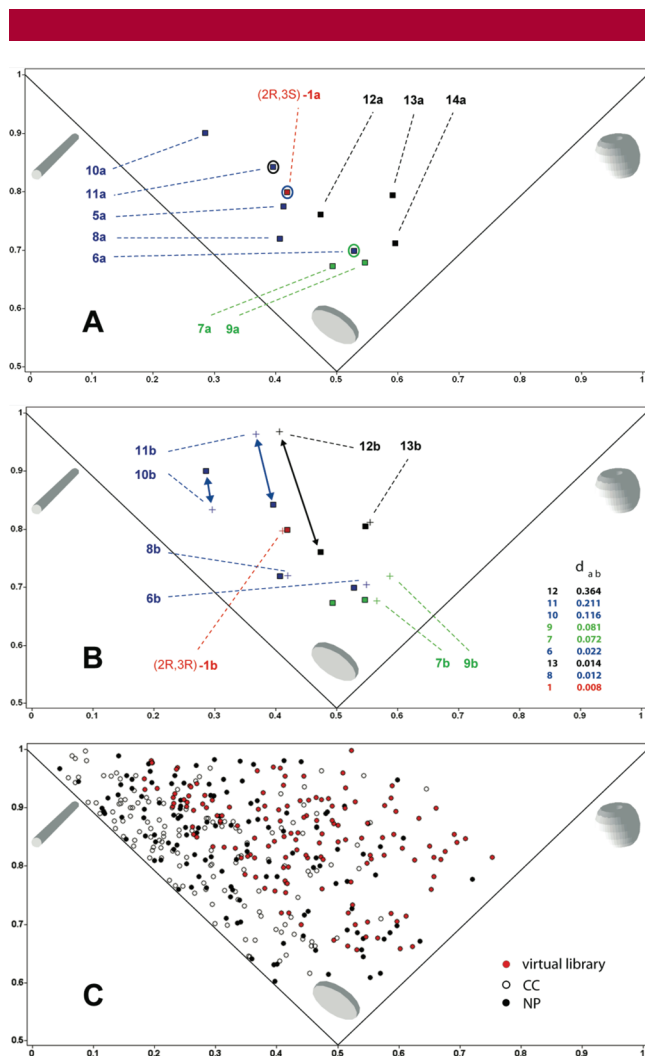


Figure 3. Molecular shape analysis. (A) PMI plot depicting relationships between compounds **1a** and **5a–14a** shown in Scheme 2. Substrate–product relationships are indicated with matched colors between product markers and circles around substrate markers. (B) PMI plot showing shape differences between diastereomeric pairs **a** (■) and **b** (+) for compounds **1** and **6–13**. Distances between pairs are listed in decreasing order, and the three most distant pairs are noted by arrows. (C) PMI plot comparing virtual library based on the Scheme 2 (see text) with subsets of molecules of different origins: commercial compounds (CC), natural products (NP).